

# RSC Advances



This is an *Accepted Manuscript*, which has been through the Royal Society of Chemistry peer review process and has been accepted for publication.

*Accepted Manuscripts* are published online shortly after acceptance, before technical editing, formatting and proof reading. Using this free service, authors can make their results available to the community, in citable form, before we publish the edited article. This *Accepted Manuscript* will be replaced by the edited, formatted and paginated article as soon as this is available.

You can find more information about *Accepted Manuscripts* in the [Information for Authors](#).

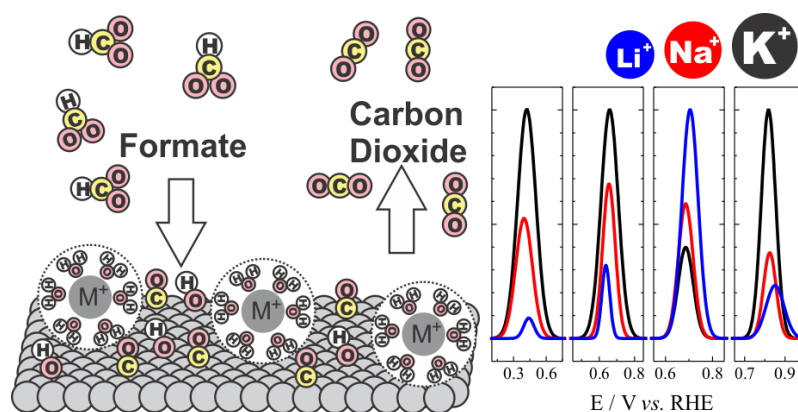
Please note that technical editing may introduce minor changes to the text and/or graphics, which may alter content. The journal's standard [Terms & Conditions](#) and the [Ethical guidelines](#) still apply. In no event shall the Royal Society of Chemistry be held responsible for any errors or omissions in this *Accepted Manuscript* or any consequences arising from the use of any information it contains.

# The effect of the alkali metal cation on the electrocatalytic oxidation of formate on platinum

Bruno A. F. Previdello,<sup>1</sup> Eduardo G. Machado,<sup>1</sup> Hamilton Varela<sup>1,2,\*</sup>

<sup>1</sup> *Institute of Chemistry of São Carlos, University of São Paulo  
POBox 780, 13560-970, São Carlos, SP, Brazil*

<sup>2</sup> *Fritz Haber Institute of the Max Planck Society, Department of Physical Chemistry,  
Faradayweg 4-6, D-14195 Berlin, Germany*



## Abstract

Non-covalent interactions between hydrated alkali metal cations and adsorbed oxygenated species on platinum might considerably inhibit some electrocatalytic reactions. We report in this communication the effect exerted by electrolyte alkali metal cation on the electro-oxidation of formate ions on platinum. The system was investigated by means of cyclic voltammetry and chronoamperometry in the presence of electrolyte containing  $\text{Li}^+$ ,  $\text{Na}^+$ , or  $\text{K}^+$ . As already observed for other systems, the general activity towards the electro-oxidation of formate ions was found to increase in the sequence  $\text{Li}^+ < \text{Na}^+ < \text{K}^+$ . In addition, we observed that the inhibition caused by smaller cations has a peculiar potential dependence because of the multi-peaked current profile of the electro-oxidation of formate on platinum. In this respect, we have also identified a new effect caused by cation inhibition at intermediate potentials, namely a peak splitting towards the use of smaller cations. Results are discussed in connection with mechanistic aspects of this model system.

**Keywords:** formate electro-oxidation, platinum, electrocatalysis, alkali metal cations, non-covalent interactions.

\* Corresponding author: varela@iqsc.usp.br

## 33 1. Introduction

34

35 It has been recently shown that the nature of the alkali metal cation in the electrolyte  
36 severely impacts the electro-oxidation of molecules such as carbon monoxide,<sup>1</sup> ethylene  
37 glycol,<sup>2, 3</sup> glycerol,<sup>3</sup> hydrogen,<sup>4</sup> methanol,<sup>4</sup> and the reduction of oxygen.<sup>5</sup> Additionally, the  
38 potential range of the transition region between diffusion-limited reduction to oxidation of  
39 hydrogen peroxide is also dependent of the alkali cation, as stated by Mayrhofer *et al.*<sup>6</sup>

40 The importance of the so-called non-covalent interactions between hydrated alkali  
41 metal cations and adsorbed hydroxyl species on the platinum surface was brought to light by  
42 Markovic and co-workers.<sup>4</sup> The presence of  $\text{OH}_{\text{ad}}-\text{M}^+(\text{H}_2\text{O})_x$  clusters at the interface  
43 increases in the order of the hydration energy of the alkali metal M (i.e.,  $\text{Li}^+ > \text{Na}^+ > \text{K}^+ >$   
44  $\text{Cs}^+$ ) and a consequent surface blockage is observed in the same order.<sup>4</sup> For most systems, the  
45 electrocatalytic activity increases in the sequence:  $\text{Li}^+ < \text{Na}^+ < \text{K}^+ < \text{Cs}^+$ .

46 The electro-oxidation of formate ions on platinum has been studied in different  
47 contexts.<sup>7-12</sup> Osawa and co-workers<sup>8</sup> investigated the electro-oxidation of formic acid/formate  
48 in the pH range between 0 and 12 and established that formate ion is the key reactant over the  
49 whole pH window. They argued on the importance of the acid-base equilibrium on the  
50 process and observed that the closer the solution pH is of the pKa of formic acid, the greater  
51 is the oxidation current. Abruña and co-workers<sup>10</sup> have recently discussed the mechanism of  
52 formate electro-oxidation thoroughly. The authors stated that the process starts with the  
53 adsorption of a given X1 species, which is a stable adsorbate that adsorbs more weakly than  
54 formate itself. This adsorbate may react by the primary pathway, which leads directly to  $\text{CO}_2$   
55 or by the secondary pathway, in which X1 generates  $\text{CO}_{\text{ads}}$  that reacts with adsorbed  $\text{OH}^-$  to  
56  $\text{CO}_2$ . Wieckowski and co-workers<sup>7</sup> discussed the occurrence of three peaks along the  
57 potentiodynamic sweep as resulting of a triple pathway mechanism, including a third path  
58 through the oxidation of less-active adsorbate at higher potentials in addition to the well-  
59 known dual pathway. From the applied perspective, the electro-oxidation of formate ions is of  
60 utter importance, because of the increasingly interest in alkaline fuel cells.<sup>13-15</sup>

61 Motivated by the intricate multi-processes feature of the current-potential curve of the  
62 electro-oxidation of formate ions on platinum, herein we present results on the experimental  
63 investigation of the effect of the nature of the alkali metal cation in the electrolyte on this  
64 system.

65

## 66 2. Experiments and Methods

67

68 **Solutions.** All solutions were prepared with ultra-pure Millipore<sup>®</sup> water (18.2 MΩ.cm).  
69 Aqueous solutions at 0.1 M of KOH (Sigma Aldrich), NaOH (Sigma-Aldrich), or LiOH  
70 (Sigma-Aldrich) were used as electrolytes. Prior to each experiment, formic acid  
71 (Sigma-Aldrich) was added to the electrolyte solution in order to yield formate at the  
72 concentration of 0.1 M.

73 **Electrodes.** The working electrode was a polycrystalline platinum flag with geometric area of  
74 0.302 cm<sup>2</sup>. All current densities are referred to the electroactive area, as measured before each  
75 experiment by means of the hydrogen oxidation. The electrode roughness was typically about  
76 1.42. The counter electrode was a platinum net with very high surface area. The reference  
77 electrode was a reversible hydrogen electrode prepared with the supporting electrolyte, with  
78 respect to which all potentials will be referred to.

79 **Cleanness.** Since working with alkaline media demands a special attention to the cleanness of  
80 the system as to ensure the reproducibility of the results, before each experiment, a chemical  
81 cleaning was employed. All the glassware was immersed in a slightly alkaline potassium  
82 permanganate solution the day before the experiment. In the next day, it was washed with  
83 water and immersed in slightly acid hydrogen peroxide solution. Next, it was washed  
84 thoroughly with boiling ultra-pure water. After the chemical cleaning, the electrode was  
85 flame-annealed with a butane flame for about 1 minute and then cooled at argon atmosphere.  
86 Finally, it was inserted into the cell and it was performed an electrochemical annealing, with  
87 150 voltammetric cycles ranging from 0.05 V to 1.5 V at 2 V.s<sup>-1</sup>.

88 **Electrochemical Setup.** The cell used was a one-chambered cell and all experiments were  
89 performed with stagnant solution. Before and during all measurements, argon (White  
90 Martins<sup>®</sup>) was purged into the system in order to reduce oxygen dissolution. Experiments  
91 were performed at 25±1°C, controlled by a thermostat. The electrochemical measurements  
92 were accomplished using an Autolab<sup>®</sup> potentiostat (model PGSTAT302N) with the modulus  
93 Scan-Gen coupled (analog scan generator).

94 Deconvolution. The deconvolution of the voltammetric peaks was performed  
95 with the software Origin 8.6<sup>®</sup>. Initially it was drawn a baseline for the first half  
96 of the scan, in order to eliminate experimental noise and minimize the  
97 capacitance component of the total current. Next, the peaks were selected and it

98 was performed a Gaussian curve fitting. The coefficient of determination ( $R^2$ )  
99 for the fitting ranged from 0.990 to 0.996.

### 100 **3. Results and Discussion**

101

#### 102 *Cyclic Voltammetry*

103 Figure 1 displays the (a) base-cyclic voltamograms, (b) the positive-, and (c) the  
104 negative-going sweep after addition of formate ions. The base-CVs are identical to that  
105 previously reported<sup>2</sup> and the main aspect to be highlighted is the fact that the non-covalent  
106 interactions slightly postpones the surface oxidation as clearly seen along the positive and,  
107 more transparently, the negative-going sweep, where the reduction charge increase in the  
108 sequence  $\text{Li}^+ < \text{Na}^+ \sim \text{K}^+$ . As already mentioned, this observation results from the higher  
109 interfacial concentration of  $\text{OH}_{\text{ad}}-\text{M}^+(\text{H}_2\text{O})_x$  clusters accompanying the increase in the  
110 hydration energy or the decrease in the ionic radius of the alkali metal cations.<sup>4</sup> After this  
111 initial inhibition on the onset of surface oxidation, the voltammetric profiles become very  
112 similar, as the interactions between hydrated cation and the platinum surface are negligible at  
113  $E > \sim 1.0$  V. This is due to the cation repulsion at high potentials and also to the prevailing of  
114 the interaction between platinum and oxygenated species.

115

116

117

118

119

120

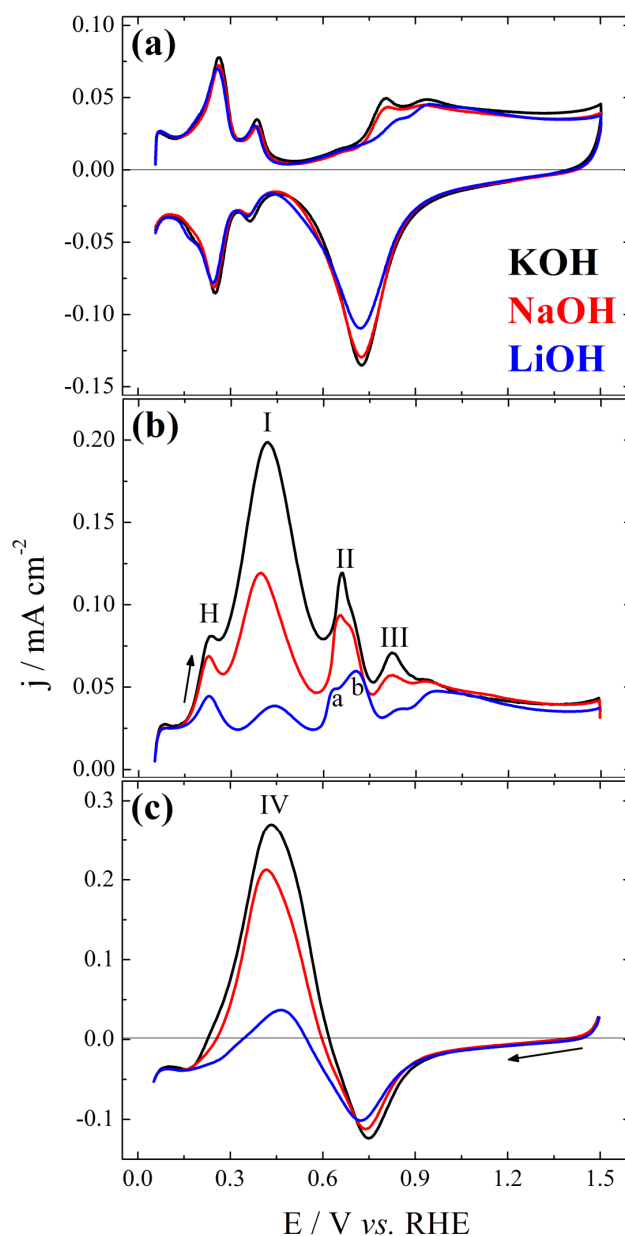
121

122

123

124

125



126  
 127 **Figure 1:** Voltammetric characterization of the platinum electrode in (a)  
 128 0.1 MOH (M = K, Na, Li); and after addition of 0.1 M  $\text{HCOO}^-$  along the (b)  
 129 positive-, and (c) negative-going sweep.  $dE/dt = 50 \text{ mV}\cdot\text{s}^{-1}$ .  
 130

131 Focusing now on the voltammetric profiles of the electro-oxidation of formate ions,  
 132 Figures 1(b) and (c), the first aspect to be highlighted is the clear activity increase in the  
 133 sequence  $\text{Li}^+ < \text{Na}^+ < \text{K}^+$ . Nevertheless, unlike the similar effect observed for methanol,<sup>4</sup>  
 134 ethylene glycol,<sup>2</sup> and glycerol,<sup>3</sup> the highly structured or multi-peaked curve observed here  
 135 makes the effect more intricate. Peak H in Figure 1(b) can be mainly assigned to hydrogen  
 136 desorption and it is considerably inhibited by the presence of  $\text{Li}^+$ , and also of  $\text{Na}^+$  to a lesser  
 137 extent. Following the notation used by Wieckowski and co-workers,<sup>7</sup> peaks I, II, and III are  
 138 assigned in Figure 1(b). As further discussed below, peak II is clearly divided into *a* and *b* as

139 a smaller cation is used. Peak I has been commonly accepted as relative to the direct oxidation  
140 of formate to  $\text{CO}_2$  without forming  $\text{CO}_{\text{ad}}$  as intermediate.<sup>7, 10</sup> The activity decrease observed  
141 here can be simply related to the decrease in the surface sites for the adsorption of the initial  
142 active intermediate, due to the presence of  $\text{OH}_{\text{ad}}-\text{M}^+(\text{H}_2\text{O})_x$  clusters. Peak II have been  
143 assigned to the electro-oxidation of adsorbed carbon monoxide in the indirect pathway.<sup>7, 10</sup> In  
144 that pathway, an intermediate of formate adsorbs and yields  $\text{CO}_{\text{ad}}$  that reacts with  $\text{OH}_{\text{ad}}$  to  
145  $\text{CO}_2$ .

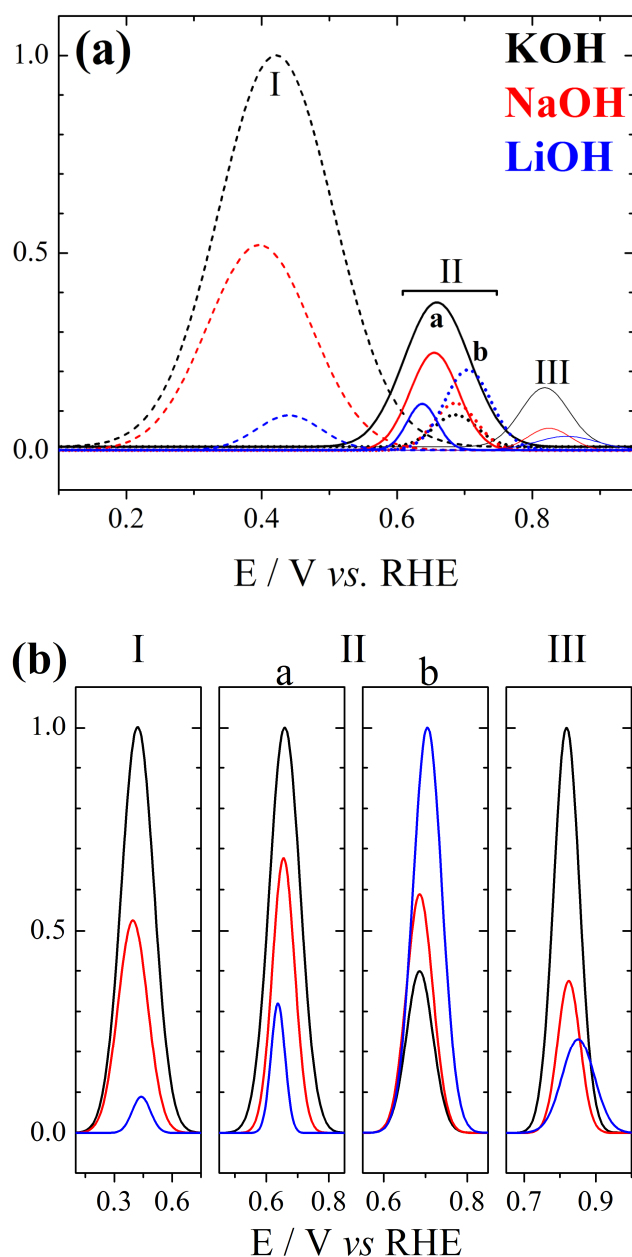
146 In the modified triple-path scheme, Wieckowski and collaborators<sup>7</sup> suggest a third  
147 pathway around peak III, completely independent of the two other pathway, involving a less  
148 active adsorbate. The fact that peak III is apparently suppressed in the presence of  $\text{Li}^+$ , as  
149 suggested by the coincidence in the initial surface oxidation in Figures 1(a) and (b), is  
150 apparently similar to the facilitated  $\text{CO}_{\text{ad}}$  oxidation as presented by Koper and co-workers.<sup>1</sup>  
151 The promoting effect is caused by the early adsorption of OH species on the platinum, which  
152 favors the oxidation of  $\text{CO}_{\text{ad}}$ . In the case of  $\text{Li}^+$ , the authors observed that oxidation does not  
153 start earlier but it is rather completed at a lower potential, as compared to the situation with  
154  $\text{Na}^+$  and  $\text{K}^+$ .<sup>1</sup> Wieckowski *et al.*<sup>7</sup> suggested that the electro-oxidation of this less active  
155 adsorbate would also proceed via a Langmuir-Hishelwood step with an adsorbed oxygenated  
156 species. Therefore, a similar effect could be operative here. Further experiments, in particular  
157 with well-defined surfaces under comparable conditions, would be needed to clarify this  
158 point.

159 Figure 1(c) shows the negative-going sweep that follows the forward scan presented in  
160 part (b). Peak IV can be primarily related to process observed in peak I,<sup>7</sup> but it is also  
161 influenced by the autocatalytic production of free platinum sites along oxide reduction.<sup>16</sup> The  
162 effect of the alkali metal cation on the oxide formation along the positive going sweep is  
163 clearly seen in the reduction process characterized by the cathodic peak around 0.75 V.  
164 Indeed, the reduction charge increases in the sequence  $\text{Li}^+ < \text{Na}^+ < \text{K}^+$ , in the same way than  
165 seen in base electrolyte, Figure 1(a). Once the platinum oxides are reduced, the cation  
166 inhibition starts playing a role again, as clearly seen in the increase of peak IV, and also in the  
167 potential at which the current becomes positive along the negative-going sweep.

168 Figure 2 shows the deconvolution of the current structures presented along the  
169 positive-going sweep in Figure 1(b). The activity trend  $\text{K}^+ > \text{Na}^+ > \text{Li}^+$  is followed for peaks I,  
170 IIa, and III. The situation changes for peak IIb: the relative size between peaks IIa and IIb  
171 decrease in the sequence  $\text{K}^+ > \text{Na}^+ > \text{Li}^+$ , and it becomes smaller than 1 for LiOH electrolyte.  
172 Interestingly, the increase in peak IIb seems correlated with the decrease in peak III, in line

173 with the anticipation of the oxidation process in peak III or its earlier completion as caused by  
 174 smaller cations.

175



176 **Figure 2:** (a) Deconvolution normalized by the higher peak (KOH peak I) of the  
 177 positive-going sweep profiles presented in Figure 1(b). (b) Comparison of  
 178 normalized deconvoluted peaks.  
 179

### 180 *Chronoamperometry*

181 Additionally to the voltammetric investigation just presented, the system was studied  
 182 by chronoamperometry in order to clarify the role of the non-covalent interaction of alkali  
 183 metal cations under quasi-stationary regime. Current-time evolutions were monitored at

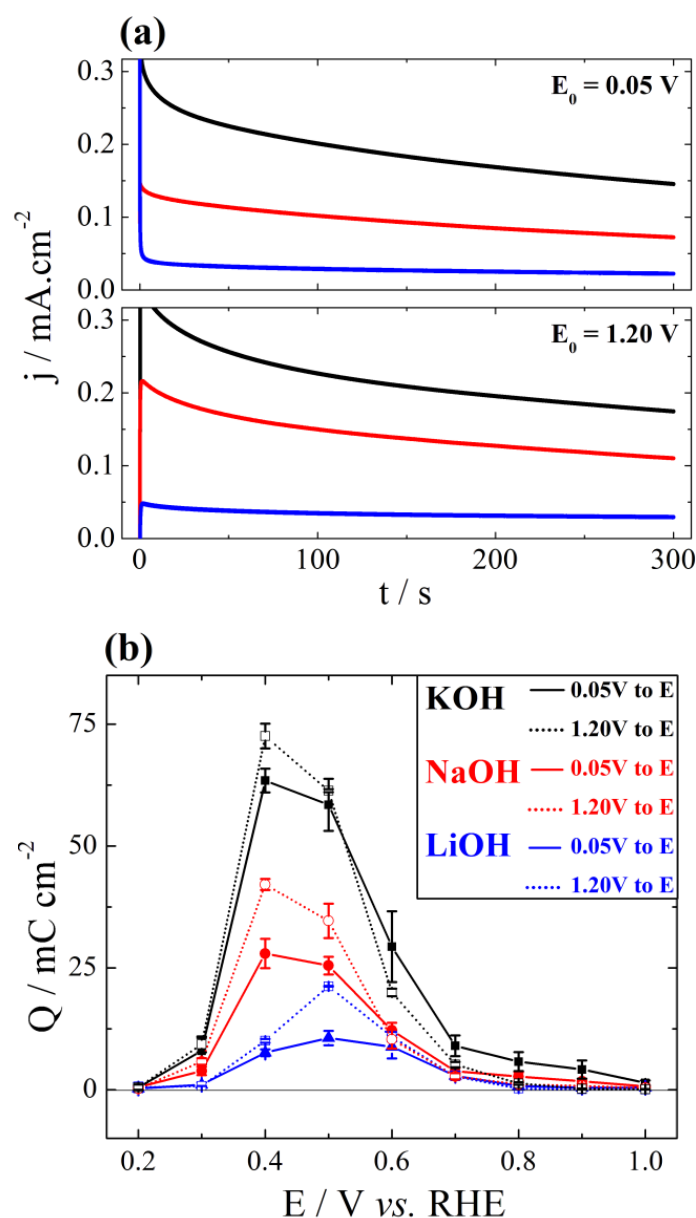


184 different potentials after a potential step from a certain initial value. This initial potential,  $E_0$ ,  
185 was either 0.05 V or 1.20 V. Figure 3(a) shows typical current profiles at  $E = 0.40$  V for three  
186 electrolytes and for two initial potentials. Figure 3(b) summarizes the total oxidation charge,  
187 i.e.  $0 < t < 300$  s, for all experiments. The activity trend follows what have been observed in the  
188 cyclic voltammograms in Figure 1(b) and (c). The first aspect to be discussed here is that, in  
189 almost all cases, the overall activity is higher when the electrode is initially polarized at  
190 1.20 V. In fact, at such high potential the surface is nearly free of carbonaceous poison<sup>17</sup> but  
191 also from  $\text{OH}_{\text{ad}}-\text{M}^+(\text{H}_2\text{O})_x$  clusters. As a consequence, the inhibition caused by smaller  
192 hydrated cations is less pronounced when the initial potential is 1.20 V. For  $E_0 = 0.05$  V, the  
193 surface started already poisoned by carbonaceous fragments and  $\text{OH}_{\text{ad}}-\text{M}^+(\text{H}_2\text{O})_x$  clusters.

194 When compared to the voltammetric profiles provided in Figure 1(b), it turns out to be  
195 clearer in Figure 3(b) that the cation inhibition becomes less important as the potential  
196 increases. Similarly to that discussed above for the base-CV, this is due to the weaker  
197 interaction between cations and positively charged surface. Although expected, this trend  
198 becomes even more transparent here because of the three discernible oxidation peaks. Finally,  
199 it is also noteworthy that the maximum activity, irrespective to the initial potential, occurs at  
200 0.40 V for solutions containing  $\text{Na}^+$  and  $\text{K}^+$ , and at 0.50 V for  $\text{Li}^+$ . This effect further  
201 evidences the dependence interfacial concentration of  $\text{OH}_{\text{ad}}-\text{M}^+(\text{H}_2\text{O})_x$  clusters on the nature  
202 of alkali cation and on the electrode potential.

203  
204  
205  
206  
207  
208  
209  
210  
211  
212  
213  
214  
215  
216  
217

218



219

220

**Figure 3:** Charges of chronoamperometric experiments. (a) chronoamperometry at  $E = 0.40$  V.  $E_0$  refers to polarization pre-measurement. (b) Comparison between two distinct pre-treatments. Full-line: Polarization in 0.05 V for 15 s and step to target potential. Dotted-line: Polarization in 1.2 V for 15 s and step to target potential.

226

227 There is an increasingly interest in the electro-oxidation of small organic molecules in  
 228 alkaline media mainly motivated by the recent development in alkaline fuel cells.<sup>13, 18</sup> The  
 229 capital role exerted by the nature of the alkali metal cation present in the electrolyte has been  
 230 demonstrated for a number of systems.<sup>1-6, 19</sup> The intricate dependence of cation blockage on  
 231 the electrode potential evidenced here for this relatively simple model-system expands the  
 232 knowledge on this relatively recently discovered phenomena. As further evidenced by some

233 intriguing kinetic aspects found under oscillatory regime in alkaline media and not yet  
234 understood,<sup>20-23</sup> there are still key questions to be answered from fundamental perspective to  
235 allow rational design of practical systems.

236

#### 237 **4. Conclusions**

238

239 The electrocatalytic oxidation of formate ions on polycrystalline platinum was  
240 investigated in the presence of different alkali metal cations. The activity was found to  
241 strongly depend on the cation dissolved in the electrolyte and it generally increases in the  
242 sequence:  $\text{Li}^+ < \text{Na}^+ < \text{K}^+$ . This trend has been found in other systems and it has been  
243 attributed to the surface blockage caused by non-covalent interactions between hydrated alkali  
244 metal cations and adsorbed oxygenated species on platinum. Peculiar to the electro-oxidation  
245 of formate ions, however, was the intricate inhibition caused by the broad and multi-peaked  
246 current-potential features. In particular, the use of smaller cations promoted a splitting of one  
247 oxidation peak at intermediate potentials and probably anticipated the oxidation of highly  
248 stable adsorbate.

249

#### 250 **Acknowledgements**

251 EGM, BAP and HV acknowledge São Paulo Research Foundation (FAPESP) for financial  
252 support (grants #2009/07629-6, #2012/07313-1, #2012/24152-1, and #2012/21204-0). HV  
253 (#306151/2010-3) acknowledges Conselho Nacional de Desenvolvimento Científico e  
254 Tecnológico (CNPq) for financial support.

255

#### 256 **References**

- 257 1. C. Stoffelsma, P. Rodriguez, G. Garcia, N. Garcia-Araez, D. Strmcnik, N. M.  
258 Marković and M. T. M. Koper, *J. Am. Chem. Soc.*, 2010, **132**, 16127.
- 259 2. E. Sitta, B. C. Batista and H. Varela, *Chem. Commun.*, 2011, **47**, 3775.
- 260 3. C. A. Angelucci, H. Varela, G. Tremiliosi-Filho and J. F. Gomes, *Electrochem.*  
261 *Commun.*, 2013, **33**, 10.
- 262 4. D. Strmcnik, K. Kodama, D. Van Der Vliet, J. Greeley, V. R. Stamenkovic and N. M.  
263 Marković, *Nat. Chem.*, 2009, **1**, 466.
- 264 5. D. Strmcnik, D. F. van der Vliet, K. C. Chang, V. Komanicky, K. Kodama, H. You,  
265 V. R. Stamenkovic and N. M. Marković, *J. Phys. Chem. Lett.*, 2011, **2**, 2733.
- 266
- 267
- 268
- 269

- 270  
271 6. I. Katsounaros and K. J. Mayrhofer, *ChemComm*, 2012, **48**, 6660.  
272  
273 7. J. Jiang, J. Scott and A. Wieckowski, *Electrochim. Acta*, 2013, **104**, 124.  
274  
275 8. J. Joo, T. Uchida, A. Cuesta, M. T. Koper and M. Osawa, *J. Am. Chem. Soc.*, 2013,  
276 **135**, 9991.  
277  
278 9. P. A. Christensen and D. Linares-Moya, *J. Phys. Chem. C*, 2010, **114**, 1094.  
279  
280 10. J. John, H. Wang, E. D. Rus and H. D. Abruña, *J. Phys. Chem. C*, 2012, **116**, 5810.  
281  
282 11. R. A. Munson, *J. Electrochem. Soc.*, 1964, **111**, 372.  
283  
284 12. P. A. Christensen, A. Hamnett and D. Linares-Moya, *PCCP*, 2011, **13**, 11739.  
285  
286 13. E. Antolini and E. R. Gonzalez, *J. Power Sources*, 2010, **195**, 3431.  
287  
288 14. A. M. Bartrom, J. Ta, T. Q. Nguyen, J. Her, A. Donovan and J. L. Haan, *J. Power*  
289 *Sources*, 2013, **229**, 234.  
290  
291 15. Y. Y. Gao, C. H. Tan, Y. P. Li, J. Guo and S. Y. Zhang, *Int. J. Hydrogen Energy*,  
292 2012, **37**, 3433.  
293  
294 16. B. C. Batista and H. Varela, *J. Phys. Chem. C*, 2010, **114**, 18494.  
295  
296 17. C. A. Angelucci, H. Varela, E. Herrero and J. M. Feliu, *J. Phys. Chem. C.*, 2009, **113**,  
297 18835.  
298  
299 18. J. Jiang and A. Wieckowski, *Electrochem. Commun.*, 2012, **18**, 41.  
300  
301 19. B. B. Berkes, G. Inzelt, W. Schuhmann and A. S. Bondarenko, *J. Phys. Chem. C*,  
302 2012, **116**, 10995.  
303  
304 20. C. P. Oliveira, N. V. Lussari, E. Sitta and H. Varela, *Electrochim. Acta*, 2012, **85**, 674.  
305  
306 21. E. Sitta, R. Nagao and H. Varela, *PLOS ONE*, 2013, **8**.  
307  
308 22. E. Sitta, M. A. Nascimento and H. Varela, *PCCP*, 2010, **12**, 15195.  
309  
310 23. E. Sitta and H. Varela, *Electrocatal.*, 2010, **1**, 19.  
311  
312  
313